Development/Plasticity/Repair

Cystine/Glutamate Exchange Modulates Glutathione Supply for Neuroprotection from Oxidative Stress and Cell Proliferation

Andy Y. Shih,[1,2] **Heidi Erb,**[1,2] **Xiaojian Sun,**[1,2] **Shigenobu Toda,**[4] **Peter W. Kalivas,**[4] **and Timothy H. Murphy**[1,2,3]

[1]Kinsmen Laboratory of Neurological Research and Brain Research Center, and Departments of [2]Psychiatry and [3]Physiology, University of British Columbia, Vancouver, British Columbia, Canada V6T 1Z3, and [4]Department of Neurosciences, Medical University of South Carolina, Charleston, South Carolina 29425

The cystine/glutamate exchanger (xCT) provides intracellular cyst(e)ine for production of glutathione, a major cellular antioxidant. Using xCT overexpression and underexpression, we present evidence that xCT-dependent glutathione production modulates both neuroprotection from oxidative stress and cell proliferation. In embryonic and adult rat brain, xCT protein was enriched at the CSF– brain barrier (i.e., meninges) and also expressed in the cortex, hippocampus, striatum, and cerebellum. To examine the neuroprotective role of xCT, various non-neuronal cell types (astrocytes, meningeal cells, and peripheral fibroblasts) were cocultured with immature cortical neurons and exposed to oxidative glutamate toxicity, a model involving glutathione depletion. Cultured meningeal cells, which naturally maintain high xCT expression, were more neuroprotective than astrocytes. Selective xCT overexpression in astrocytes was sufficient to enhance glutathione synthesis/release and confer potent glutathione-dependent neuroprotection from oxidative stress. Moreover, normally nonprotective fibroblasts could be re-engineered to be neuroprotective with ectopic xCT overexpression indicating that xCT is a key step in the pathway to glutathione synthesis. Conversely, astrocytes and meningeal cells derived from sut/sut mice (xCT loss-of-function mutants) showed greatly reduced proliferation in culture attributable to increased oxidative stress and thiol deficiency, because growth could be rescued by the thiol-donor β-mercaptoethanol. Strikingly, sut/sut mice developed brain atrophy by early adulthood, exhibiting ventricular enlargement, thinning of the cortex, and shrinkage of the striatum. Our results indicate that xCT can provide neuroprotection by enhancing glutathione export from non-neuronal cells such as astrocytes and meningeal cells. Furthermore, xCT is critical for cell proliferation during development *in vitro* and possibly *in vivo*.

Key words: xCT; system x_c^-; Nrf2; phase 2 detoxification enzymes; oxidative glutamate toxicity; cystine deprivation; meninges; oxidative stress; neuroprotection; neurogenesis

Introduction

The major cellular antioxidant glutathione (GSH) is an important line of defense against oxidative stress, and its deficiency can sensitize the brain to injury (Meister and Anderson, 1983; Mizui et al., 1992; Bobyn et al., 2002). GSH synthesis is limited by availability of the sulfhydryl amino acid cysteine, which is readily oxidized to cystine in the extracellular milieu of the brain. High-affinity cystine uptake by the Na^+-independent cystine–glutamate exchange transporter (system x_c^-) is a rate-limiting step for

GSH synthesis in various brain cell types (Miura et al., 1992). In particular, fetal brain cells (Sagara et al., 1993a), immature cortical neurons (Murphy et al., 1990), oligodendrocyte precursors (Back et al., 1998), HT22 hippocampal cell line (Li et al., 1997), and gliomas (Chung et al., 2005) are uniquely vulnerable to cystine deprivation or competitive inhibition of system x_c^- by excessive extracellular glutamate concentrations (oxidative glutamate toxicity). Prolonged oxidative glutamate toxicity leads to gradual GSH depletion, oxidative stress, and apoptosis (Ratan et al., 1994).

Structurally, system x_c^- is composed of a light-chain subunit (xCT, encoded by the *Slc7a11* gene), which confers substrate specificity (Sato et al., 1999), and a glycosylated heavy-chain subunit (4F2hc or rBAT) common to the transporter family (Mastroberardino et al., 1998; Wang et al., 2003). Basal xCT expression is highest at the CSF and blood–brain barrier, suggesting a role in redox buffering of the CSF and plasma (Sato et al., 2002). Importantly, xCT is also expressed in neurons and astrocytes of the cerebral cortex (Pow, 2001; Melendez et al., 2005; Burdo et al., 2006) and may contribute to the coupling of GSH and other sulfhydryl species between these cell types. Enhancement of as-

trocyte–neuron GSH coupling is coordinated by the stress-inducible transcription factor Nrf2, which upregulates xCT and other GSH synthesis/release machinery to constitute a defense mechanism against oxidative stress (Sasaki et al., 2002; Shih et al., 2003). In this GSH coupling pathway, astrocytes use xCT and other transport mechanisms to uptake cyst(e)ine for GSH synthesis (Cho and Bannai, 1990; Dringen et al., 2000; Wang and Cynader, 2000; Allen et al., 2002). GSH is then exported from astrocytes and degraded back to cysteine in the extracellular space for neuronal uptake. Mature neurons primarily uptake cysteine using system x_{AG} (cysteine-permeable, Na^+-dependent glutamate transporter) (Shanker et al., 2001; Chen and Swanson, 2003), whereas immature neurons exclusively uptake cystine via xCT (Murphy et al., 1990).

Although xCT function may be essential for GSH production by individual brain cell types, its role in GSH coupling within heterogeneous neuron–astrocyte populations is unknown. Furthermore, the role of xCT has been difficult to conclusively study because its antagonist pharmacology can overlap with glutamate receptors (Patel et al., 2004). Here, we tested the hypothesis that enhanced xCT activity is sufficient to confer neuroprotection by promoting GSH synthesis and delivery from non-neuronal support cells (astrocytes and meningeal cells) to immature neurons. Conversely, we examined whether brain cells derived from sut/sut mice, which express nonfunctional xCT, experience increased oxidative stress because of chronic impairment of cystine uptake.

Materials and Methods

Materials. All chemicals were purchased from Sigma Canada (Oakville, Ontario, Canada) unless stated otherwise.

Mammalian cell culture. All experiments were approved by the University of British Columbia Animal Care Committee and were conducted in strict accordance with guidelines set by the Canadian Council on Animal Care. All rats were obtained from the University of British Columbia Animal Care Facility. Enriched astrocyte cultures were prepared from the cerebral cortices of postnatal day 0 (P0) to P2 Wistar rat pups using the papain dissociation method, as described previously (Shih et al., 2003). Enriched meningeal cultures from leptomeninges of P0–P2 Wistar rat pup brains (collected from the surface of cerebral and cerebellar cortices) and fibroblast cultures from the eviscerated bodies of embryonic day 18 (E18) Wistar rat fetuses (head removed) were similarly prepared using the papain dissociation method. All non-neuronal cell types were grown in culture for 7 d and used for experiments before 10 d *in vitro* (DIV). The various non-neuronal cells had different growth rates, with fibroblasts and meningeal cells proliferating approximately three times faster than astrocytes, based on MTT [(2)-3-(4,5-dimethylthiazol-2-yl)-2,5-diphenyl-2*H*-tetrazolium bromide] turnover and protein concentrations assays. Therefore, when comparing neuroprotection by non-neuronal cells, we seeded astrocytes at a three times higher density to achieve comparable cell densities at the time of glutamate exposure.

Immature cortical cultures were prepared from the cerebral cortices of E18 Wistar rat fetuses, as described in detail previously (Shih et al., 2003). Importantly, immature cortical cultures were first plated in B27-supplemented Neurobasal medium (NBM) at 1×10^6 cells/ml (Invitrogen, Gaithersburg, MD) to ensure neuronal health at an early stage. After 1 DIV, NBM was exchanged for minimum essential medium (MEM; Invitrogen) supplemented with 5.5 g/L D-glucose, 2 mM glutamine, 10% fetal bovine serum (FBS; HyClone, Logan, UT), 1 mM pyruvate, 100 U/ml penicillin, and 0.1 mg/ml streptomycin (MEM-pyr). This medium change was required to reduce excessive antioxidant levels from the B27-supplemented medium for subsequent oxidative challenge. At neuronal age 2 DIV, various non-neuronal cell types (collected 24 h after infection with adenovirus, for some experiments) were trypsinized and transplanted directly into naive (no contact with virus) immature cortical cultures. Buthionine sulfoximine (BSO) experiments in neuron–astrocyte coculture required a setup in which astrocytes were physically sepa-

rated from neurons. This setup consisted of naive immature cortical cultures (2 DIV) prepared in 24-well plates and infected astrocytes separated in collagen-coated culture plate inserts (Millipore, Bedford, MA), as described in detail previously (Shih et al., 2003). At 3 DIV, toxicity treatments were initiated (see below). At 4 DIV, the cocultures were washed and fixed for quantification of neuronal viability (see below).

Human embryonic kidney 293 cells (HEK293; American Type Culture Collection, Manassas, VA) were grown and transiently transfected as described previously (Shih et al., 2003).

Plasmids and adenoviral constructs and infections. Recombinant adenoviral vectors were constructed using the Cre-lox system (Canadian Stroke Network core facility, University of Ottawa, Ottawa, Ontario, Canada) (Hardy et al., 1997). Briefly, the mouse xCT cDNA (a gift from Dr. S. Bannai, University of Tsukuba, Tsukuba, Japan) was excised from the pcDNA3.1+ vector using the restriction enzymes *Not*I and *Eco*RI (Sato et al., 1999; Shih and Murphy, 2001). The cDNA was then subcloned into the adenovirus construct. C-terminal epitope-tagged xCT (HA-xCT) was generated by subcloning the xCT cDNA upstream and in frame with the hemagglutinin (HA) coding sequence within the GW1 vector (a gift from Dr. A. el-Husseini, University of British Columbia) using the *Hin*dIII and *Eco*RI restriction enzymes in the vector. Infections were performed as described previously (Shih et al., 2003). In this study, a multiplicity of infection of 200 plaque-forming units/cell was used. All viruses carried a green fluorescent protein (GFP) cDNA driven by its own cytomegalovirus promoter for monitoring of viral infection.

Toxicity treatment. For all toxicity studies, the cortical cultures were used in their immature state (<4 DIV) when a full complement of ionotropic glutamate receptors was not yet expressed. Previous control studies confirmed that NMDA receptor-dependent excitotoxicity is not involved in the oxidative glutamate toxicity paradigm (Shih et al., 2003). MEM-pyr was replaced with MEM supplemented with 5.5 g/L D-glucose, 2 mM glutamine, 5% FBS, 100 U/ml penicillin, and 0.1 mg/ml streptomycin (MEM–5% FBS) containing the indicated concentrations of L-glutamate or H_2O_2. Cells were exposed to all toxins for 24 h before evaluation of neuronal viability.

Determination of neuronal viability. Immature cortical cultures were immunostained with antibodies for anti-neuron-specific enolase (NSE), followed by Texas Red-conjugated secondary antibodies (see below). Neuronal viability was evaluated by manual counting of cells positively labeled for NSE, as described previously (Shih et al., 2003).

xCT antibody production. The rabbit xCT polyclonal antibody was generated using a synthetic eight-branch multiple antigen peptide corresponding to a 15 aa sequence in the N-terminal region of the mouse xCT protein (VATISKGGYLQGNMS) (Szumlinski et al., 2004). Animals were immunized five times, and the final antiserum was purified by affinity-column chromatography using the original peptide. xCT-specific bands were absent in blots probed with preimmune serum and when the antibody was preadsorbed with peptide (data not shown).

Western blot analysis and immunocytochemistry. Cell cultures were washed with PBS, collected in harvest buffer containing PBS with a commercial mixture of protease inhibitors (Roche Biochemicals, Burlington, NC), and sonicated for 10 s to make a crude lysate. For tissue collection from E18 rat brains, leptomeninges were first taken from the surface of the cerebral and cerebellar cortices. Major brain regions were then dissected out using tweezers. Tissue collection from adult rats was similar, except the entire brain was sliced into 1-mm-thick coronal sections to aid identification of structures. All tissue samples were collected on ice and homogenized in harvest buffer with 10 strokes of a Dounce homogenizer. For Western blot-positive controls, astrocyte cell lysates were collected 24 h after infection with Ad-xCT or Ad-Nrf2. Protein concentration was measured using the bicinchonic acid method (Pierce, Rockford, IL). Samples diluted in loading buffer (7 mg/ml dithiothreitol, 5% β-mercaptoethanol (β-ME), 6% SDS, 30% glycerol, 0.38 M Tris, pH 6.8, and pyronin Y) were denatured by boiling for 2 min before gel loading. Dithiothreitol and β-ME were omitted from the loading buffer for nonreducing conditions. For SDS-PAGE, 10% acrylimide gels were used to run all samples at 10 μg per lane. Antibody reactivity was detected using ECL chemiluminscence substrate (Amersham Biosciences, Piscataway, NJ).

For immunocytochemistry after toxicity experiments, cultures were washed three times with 37°C PBS and fixed with 2% paraformaldehyde for 10 min. Fixed cells were washed three times and incubated with primary antibodies overnight, followed by fluorescent secondary antibodies for 1 h at room temperature. Immunostained cells were washed three times and mounted in Fluoromount-G (Southern Biotechnology, Birmingham, AL).

The antibodies used in this study include the following: anti-GFP from mouse (1:1000; Boehringer Mannheim, Indianapolis, IN), anti-NSE from rabbit (1:2000; Polysciences, Warrington, PA), anti-mouse Alexa Fluor 488 from goat (1:2000; Invitrogen), anti-rabbit Texas Red from goat (1:2000; Invitrogen), anti-actin from goat (1:1000; Santa Cruz Biotechnology, Santa Cruz, CA), anti-HA (1:1000; Babco, Berkeley, CA), anti-xCT (1:250; custom made), anti-4F2hc (1:100; Santa Cruz Biotechnology), anti-rabbit horseradish peroxidase (HRP) from sheep (1:5000; Amersham Biosciences), anti-mouse HRP from sheep (1:5000; Amersham Biosciences), and anti-goat HRP from donkey (1:5000; Santa Cruz Biotechnology)

Total intracellular GSH assay and effluxed GSH assay. Total intracellular and media GSH was quantified by the method of Tietze (1969). These methods were described in detail previously (Shih et al., 2003). The monochlorobimane (mCBi) (Invitrogen) plate reader assay of GSH content in astrocytes and meningeal cells was performed as described previously (Sun et al., 2005).

Radioactive substrate uptake assays. xCT uptake activity was measured in cultured cells as described previously (Shih and Murphy, 2001; Shih et al., 2003). Briefly, cultures were preincubated in Na⁺-free HBSS for 10 min at 37°C and then incubated with Na⁺-free HBSS containing 1.6 Ci/ml L-[^{3}H]glutamate or 1 Ci/mL L-[^{35}S]cystine (Amersham Biosciences) and the indicated concentrations of any unlabeled competitors for an additional 20 min at 37°C. Then the cells were washed three times with ice-cold Na⁺-free HBSS and lysed with 0.5% Triton X-100 in 0.1 M phosphate buffer. Radioactivity was determined by liquid scintillation counting and normalized to protein concentration for each sample. For acute uptake studies, cells were papain dissociated from E18 Wistar rat meninges and cortex (with the cell culture protocol), immediately resuspended in Na⁺-free HBSS, and divided into Eppendorf tubes (1×10^6 cells/tube). The cells were pelleted at $2000 \times g$ and resuspended in 300 μl of radioactive substrate solutions for 20 min at 37°C. Cells were washed by spinning down and resuspending three times with 1 ml of ice-cold Na⁺-free HBSS and lysed with 100 μl of 0.5% Triton X-100 in 0.1 M phosphate buffer. Perchloric acid was added (3% final concentration) to separate the acid-soluble and protein fractions. The protein precipitate was removed by centrifugation ($14,000 \times g$ for 10 min), and the acid-soluble fraction (containing free amino acids and GSH) was measured for radioactivity.

Mouse colonies. sut/sut mice breeding pairs were obtained from Dr. R. Swank (Roswell Park Cancer Institute, Buffalo, NY) (Chintala et al., 2005). The C3H/HeSnJ control background strain was obtained from The Jackson Laboratory (Bar Harbor, ME). All mice were maintained at the University of British Columbia Animal Care Facility in a 12 h light/dark cycle with food and water *ad libitum*.

Brain morphology measurements. sut/sut and C3H/HeSnJ mice, ~3.5 months of age, were deeply anesthetized with euthanyl (Bimeda-MTC) and perfused transcardially with room temperature PBS, followed by ice-col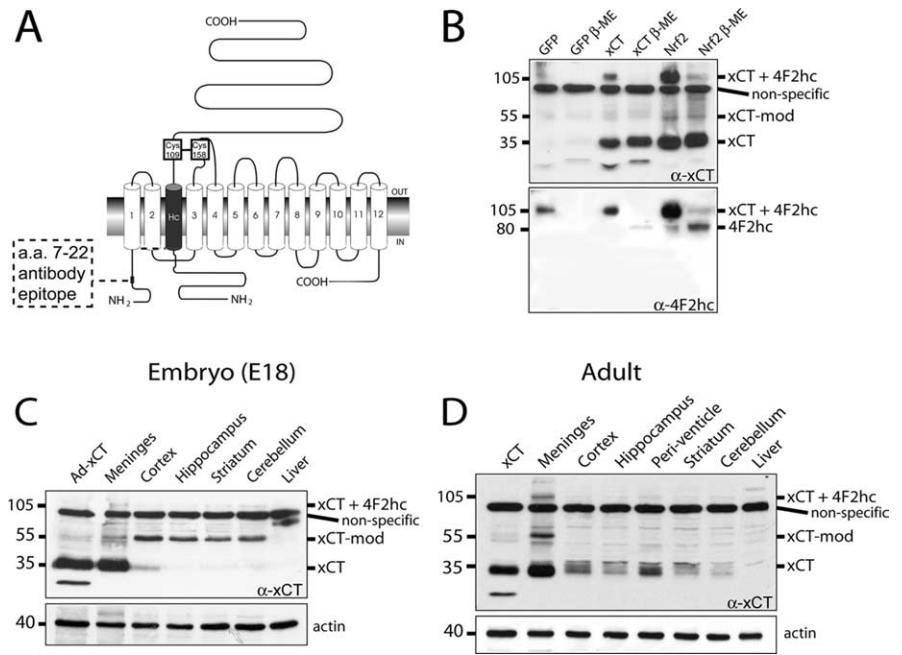d 4% paraformaldehyde in PBS. The brains were postfixed overnight in paraformaldehyde, cryoprotected with 30% sucrose for 2 d, and cryosectioned. Cresyl violet staining was performed with standard protocols on 40 μm sections mounted on SuperFrost Plus slides (Fisher Scientific, Houston, TX) and scanned at 600 dpi on a desktop scanner (Epson 1660). Brain measurements were performed on scanned images using Image J software (version 1.33u; National Institutes of Health, Bethesda, MD). Ventricle, striatum, and hippocampal areas were measured bilaterally and averaged for each bregma. The measured hippocampal area encompassed all major layers including the stratums oriens, pyramidale, radiatum, moleculare, and dentate gyrus. Cortical width was also measured bilaterally between the apex of the corpus callosum to the pial layer of the cortex (primary motor cortex region).

Statistical analysis. All experiments were repeated at least three times. Results are presented as the mean ± SEM. Statistical analysis of raw data was performed with Prism 2.0 (Graph Pad, San Diego, CA). Experimental groups were compared by one-way ANOVA, two-way ANOVA, or Student's t test (*$p < 0.05$, **$p < 0.01$, and ***$p < 0.001$).

Results

Characterization of an anti-xCT polyclonal antibody

To examine xCT protein expression in rodent brain and to validate our overexpression assays, we developed a polyclonal antibody specific for N-terminal amino acids (7–22) of the mouse xCT protein, a region predicted to be both hydrophilic and intracellular by membrane topology analysis (Fig. 1A) (Sato et al., 1999; Szumlinski et al., 2004; Melendez et al., 2005). Antibody specificity was first verified by probing astrocyte cultures overexpressing xCT (Ad-xCT) or its transcriptional regulator Nrf2 (Ad-

Figure 1. Characterization of an anti-xCT polyclonal antibody and xCT regional brain distribution. *A*, xCT and 4F2hc membrane topology depicting xCT antibody epitope. xCT and 4F2hc heterodimerize through an extracellular disulfide link that can be disrupted with the reducing agents β-mercaptoethanol and dithiothreitol, collectively referred to as β-ME. a.a., Amino acid. *B*, The anti-xCT antibody detected a major 35 kDa band and a minor 55 kDa band (xCT-mod) that was specific only to xCT and Nrf2-overexpressing astrocyte cultures. Low basal levels of the same bands were detected in the GFP-overexpressing control. The 105 kDa band seen under nonreducing conditions corresponded to the xCT plus 4F2hc heterodimer. Treatment with β-ME disrupted the disulfide link between xCT and 4F2hc, causing the 105 kDa band to disappear, shifting to monomeric 35 kDa xCT. xCT-mod could not be disrupted by reducing conditions, suggesting that it is not a disulfide-linked xCT homodimer. A strong nonspecific band was detected at 95 kDa. Stripping and reprobing with an anti-4F2hc antibody revealed the 105 kDa band (xCT + 4F2hc) under nonreducing conditions and a 80 kDa band (4F2hc only) with reducing conditions. *C*, Examination of xCT regional distribution in the embryonic rat brain revealed high expression of 35 kDa xCT and xCT-mod in the meninges, whereas all other brain regions examined express primarily xCT-mod. *D*, In the adult rat brain, 35 kDa xCT and xCT-mod was also highly expressed in the meninges. In contrast to embryonic tissues, other adult brain regions express primarily 35 kDa xCT. Blots are representative results from at least three independent experiments on separately prepared cultures or separate rats.

Nrf2) in Western blot (Sasaki et al., 2002; Shih et al., 2003). With both Ad-xCT- and Ad-Nrf2-infected cultures, the antibody detected three bands corresponding to xCT at 35, 55, and 105 kDa (Fig. 1B, top blot). These bands were barely detectable in Ad-GFP-infected controls. The 35 kDa band corresponded to the monomeric form of xCT. The 105 kDa band, which was detectable using both xCT and 4F2hc antibodies, was only present under nonreducing conditions and represented the xCT plus 4F2hc disulfide-linked heterodimer. Monomeric 4F2hc migrated at 80 kDa under reducing conditions (Fig. 1B, bottom blot) (Burdo et al., 2006). Interestingly, Nrf2 overexpression increased 4F2hc protein expression, suggesting possible xCT and 4F2hc coregulation in astrocytes (Gochenauer and Robinson, 2001). A fainter 55 kDa band (xCT-mod) was consistently detected in xCT- and Nrf2-overexpressing astrocytes but was unlikely to be an xCT homodimer because it was too low in molecular weight and could not be disrupted by reducing conditions (Fig. 1A, top blot). The density of this band was increased with xCT and Nrf2 overexpression, unlike the nonspecific band at 95 kDa, suggesting that it is derived from the xCT transcript and may be an alternatively spliced or translationally modified form distinct from 35 kDa xCT (Kim et al., 2001). No heterodimerization was observed between 4F2hc and xCT-mod.

To further verify the migration of xCT at 35 kDa and 55 kDa, we overexpressed HA-tagged xCT (HA-xCT) in HEK293 cells and examined its migration in Western blot using an HA-specific antibody. Consistent with adenoviral xCT and Nrf2 overexpression, the majority of HA-xCT was detected at 35 kDa, and a minor component was observed at 55 kDa. Furthermore, the 105 kDa HA-xCT-4F2hc heterodimer could be disrupted under reducing conditions, but not the 55 kDa band (supplemental Fig. 1A, available at www.jneurosci.org as supplemental material).

In vivo regional distribution of xCT protein

The antibody was used to determine the regional tissue distribution of xCT protein in the immature (E18) and adult rat brain by Western blot. No immunostaining was performed because of the possibility that the nonspecific 95 kDa band may interfere. In the immature brain, both 35 kDa xCT and xCT-mod were robustly expressed in the meninges (Fig. 1C) (Sato et al., 2002; Burdo et al., 2006). xCT-mod was predominantly expressed in major regions of the immature brain including the cortex, hippocampus, striatum, and cerebellum. In adult tissues, meningeal expression of 35 kDa xCT and xCT-mod remained high (Fig. 1D). However, a developmental transition in xCT protein was observed because 35 kDa xCT was now predominant in all major brain regions, whereas xCT-mod expression decreased. Consistent with mRNA analysis studies by Sato et al. (2002), high levels of xCT protein expression were observed in the adult periventricular region containing the ependymal cells of the lateral ventricles, but no protein was detected in liver.

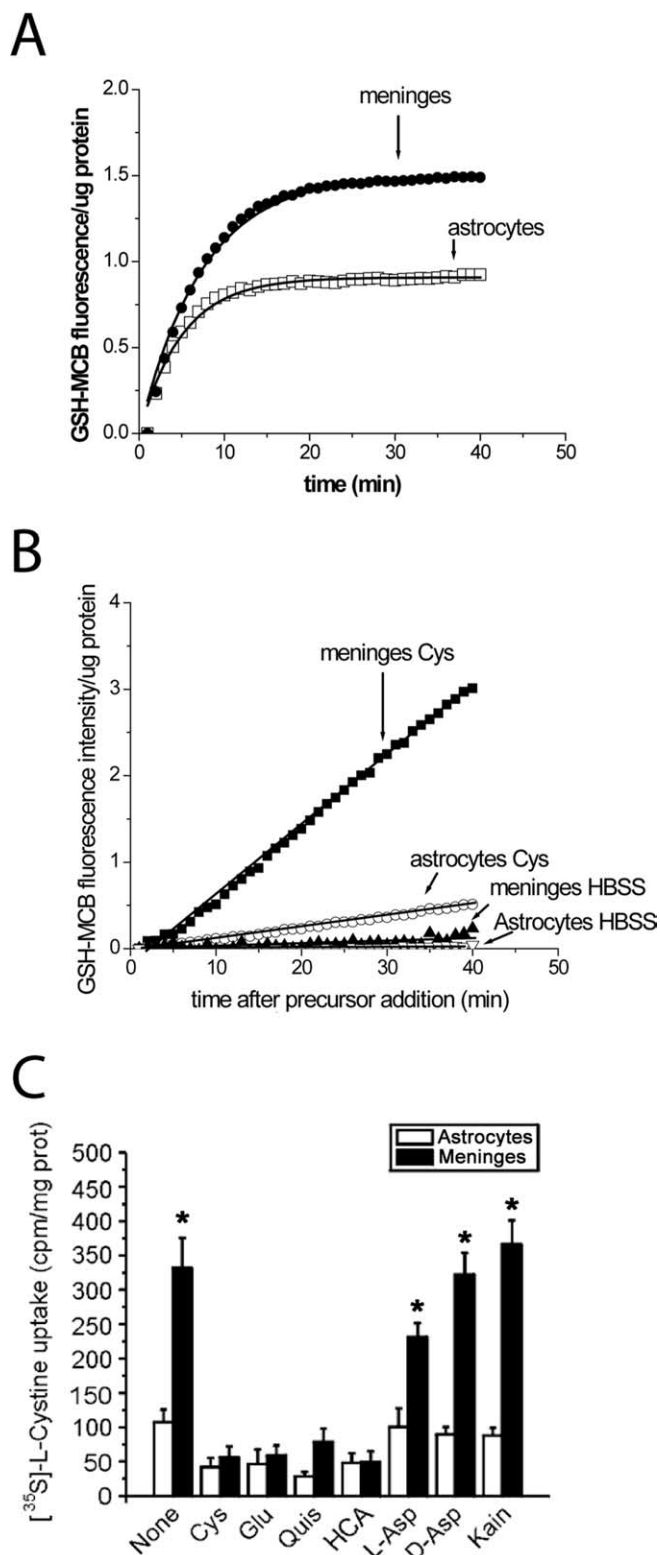Further confirming xCT transcriptional modulation by Nrf2,

Figure 2. Meningeal cells exhibit higher GSH content and enhanced cystine-dependent GSH synthesis. Characteristics of GSH metabolism in primary meningeal and astrocyte cultures were examined using a previously characterized mCBi labeling assay (Sun et al., 2005). *A*, Meningeal cells showed an increased initial slope of mCBi fluorescence labeling over time, corresponding to increased glutathione *S*-transferase activity and rate of GSH–mCBi conjugation. Importantly, a higher plateau of fluorescence in meningeal cells (after 20 min of labeling) indicates higher cellular GSH content, because GSH levels were limiting in this assay. *B*, After the fluorescence plateau was reached, the mCBi labeling assay could also be used to monitor new GSH synthesis. Application of 100 μM cystine to the culture medium generated a larger increase in GSH–mCBi fluorescence from meningeal cultures compared with astrocytes, indicating that meningeal

←

cells preferentially uptake cystine for GSH synthesis. The HBSS vehicle control had no significant effect on new GSH synthesis in either meningeal cells or astrocytes. The graphs in *A* and *B* are representative traces from at least three independent experiments. *C*, Consistent with preferential meningeal use of cystine to make GSH, Na$^+$-independent L-5^{35}-cystine uptake was threefold higher than astrocytes and fit the pharmacological profile of system x_c^-. All competitors were introduced at a concentration of 1 mM, except quisqualic acid (300 μM). Data represent the mean $\pm$ SEM from three independent experiments on separately prepared cultures. *$p < 0.05$ compared with astrocytes. Cys, L-Cystine; Glu, L-glutamate; Quis, quisqualic acid; HCA, homocysteic acid; L-Asp, L-aspartate; D-Asp, D-aspartate; Kain, kainic acid.

meningeal tissues from adult Nrf2$^{-/-}$ mice showed decreased expression of the 35 kDa xCT band, compared with wild-type littermates (supplemental Fig. 1B, available at www.jneurosci.org as supplemental material) (Chan et al., 1996; Sasaki et al., 2002). A modest reduction in xCT protein was also observed in the cortex, but not in other brain tissues examined. The expression level of xCT was also verified using Na$^+$-independent L-[^{35}S]cystine and L-[^{3}H]glutamate uptake assays (both can be used as substrates) on enzymatically dissociated E18 rat meningeal and cortical tissue. Indeed, Na$^+$-independent L-[^{35}S]cystine uptake was 23.2 ± 5.7-fold higher in meningeal cells than in cortical cells and was completely inhibited by 1 mM nonradiolabeled glutamate. L-[^{3}H]Glutamate uptake was 6.4 ± 2.1-fold higher in meningeal cells than in dissociated cortex and was completely inhibited by 1 mM nonradiolabeled cystine. The relative difference between meningeal and cortical tissues was higher when using cystine as a substrate and may have been related to higher basal levels of glutamate uptake by other transporters.

Meningeal cells exhibit enhanced GSH synthesis and neuroprotection of immature neurons

The immature brain contains high levels of GSH compared with the adult brain, which may be important for cell proliferation and neuronal viability during development (supplemental Fig. 2A,B, available at www.jneurosci.org as supplemental material) (Lowndes et al., 1994). We hypothesized that xCT-mediated GSH production could serve an important neuroprotective role in the immature brain and that augmentation of this pathway could confer increased protection from oxidative stress. We examined this possibility using relatively purified primary culture systems. Neuroprotection in culture was specifically defined as an increased viability of NSE-positive immature neurons after toxicity treatment.

Consistent with higher xCT activity in meningeal tissue, cultured meningeal cells showed enhanced maximal fluorescence (F_{max}) when assayed with a selective enzyme-linked marker for GSH, monochorobimane (mCBi) (F_{max}: meninges, 1.54 ± 0.19 vs astrocytes, 1.08 ± 0.15; *$p < 0.05$, Student's t test) (Chatterjee et al., 1999; Sun et al., 2005), indicating increased GSH content compared with cultured cortical astrocytes (Fig. 2A). Indeed, cultured meningeal cells exhibited an approximate threefold higher L-[^{35}S]cystine uptake than astrocytes. Meningeal L-[^{35}S]cystine uptake fit the pharmacological profile of system x$_c^-$ because it was strongly blocked by its competitive inhibitors L-glutamate, L-quisqualic acid, and homocysteic acid, partially blocked by L- and D-aspartate, but not blocked by kainic acid (Fig. 2C). Accordingly, application of cystine to the mCBi assay led to a more pronounced upregulation in GSH synthesis ($\sim$10-fold greater slope) in meningeal cells compared with cortical astrocytes (slope of fluorescence increase: meninges, 0.096 ± 0.018 vs astrocytes, 0.009 ± 0.002; *$p < 0.05$, Student's t test) (Fig. 2B).

In our previous studies, we found that GSH release from Nrf2-overexpressing astrocytes led to potent neuroprotection of immature neurons during oxidative glutamate toxicity (Shih et al., 2003). Meningeal cells naturally exhibit high levels of Nrf2 activity (A. Y. Shih and T. H. Murphy, unpublished observation), which may explain their high level of xCT expression, GSH content, and GSH synthesis. Thus, we reasoned that meningeal cells would be highly neuroprotective. We cocultured various densities of meningeal cells, astrocytes, and peripheral fibroblasts with immature cortical neuron cultures and exposed the cocultures to oxidative glutamate toxicity (3 mM glutamate for 24 h). Indeed, cultured meningeal cells offered widespread neuroprotection
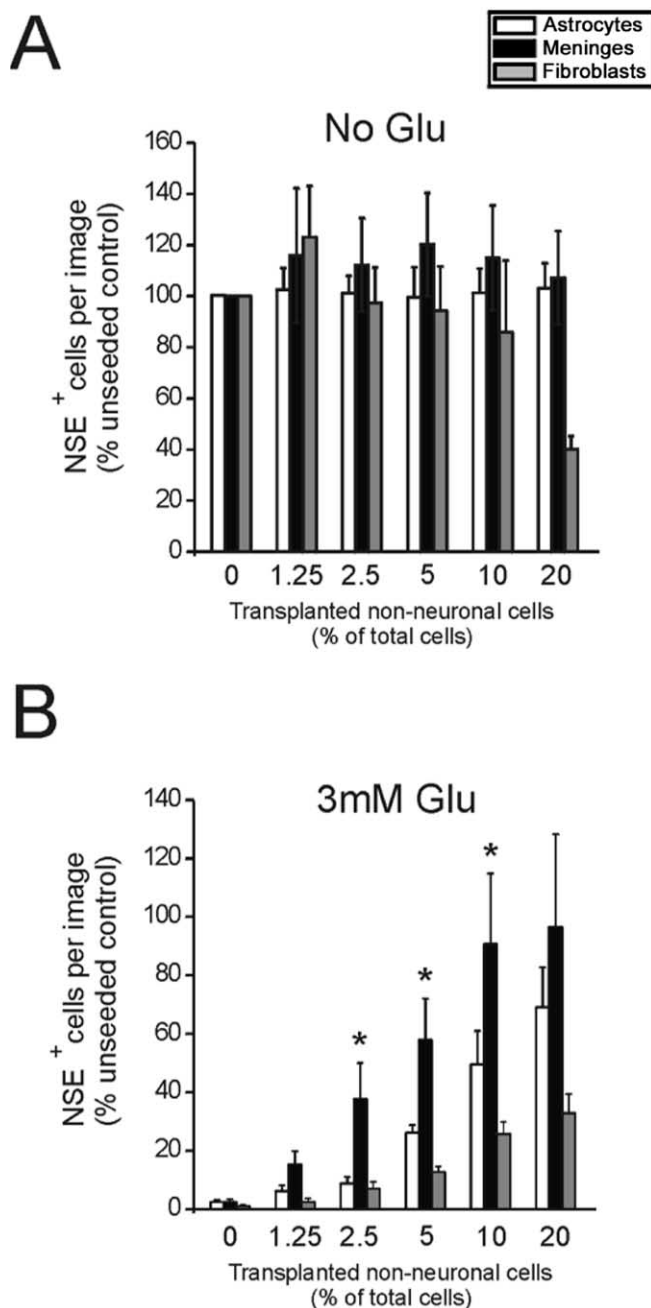

Figure 3. Meningeal cells are highly neuroprotective. Various non-neuronal cell types (meningeal cells, astrocytes, and peripheral fibroblasts) (7–10 DIV) were transplanted into immature cortical neuron cultures. To test the neuroprotective potential of each cell type, the cocultures were exposed to oxidative glutamate toxicity (*A*, *B*; 3 mM glutamate for 24 h). Meningeal cells and fibroblasts were initially seeded at a three times lower density than astrocytes because of a faster proliferation rate, so that a similar number of transplanted cells were present just before glutamate exposure (as presented on the *x*-axis). After oxidative glutamate toxicity, neurons were identified by immunocytochemistry using anti-NSE antibodies and counted. Meningeal cells conferred significantly more protection than astrocytes at a similar cell density, whereas fibroblasts were much less neuroprotective. Data represent the mean $\pm$ SEM from three independent experiments on separately prepared cultures. *$p < 0.05$ compared with astrocytes.

and were significantly more protective than astrocytes seeded at the same densities (2.5–10% of the total cell number) (Fig. 3). In contrast, peripheral fibroblasts were relatively non-neuroprotective at any plating density tested. Glutamate exposure caused no obvious meningeal cell, astrocyte, or fibroblast death.
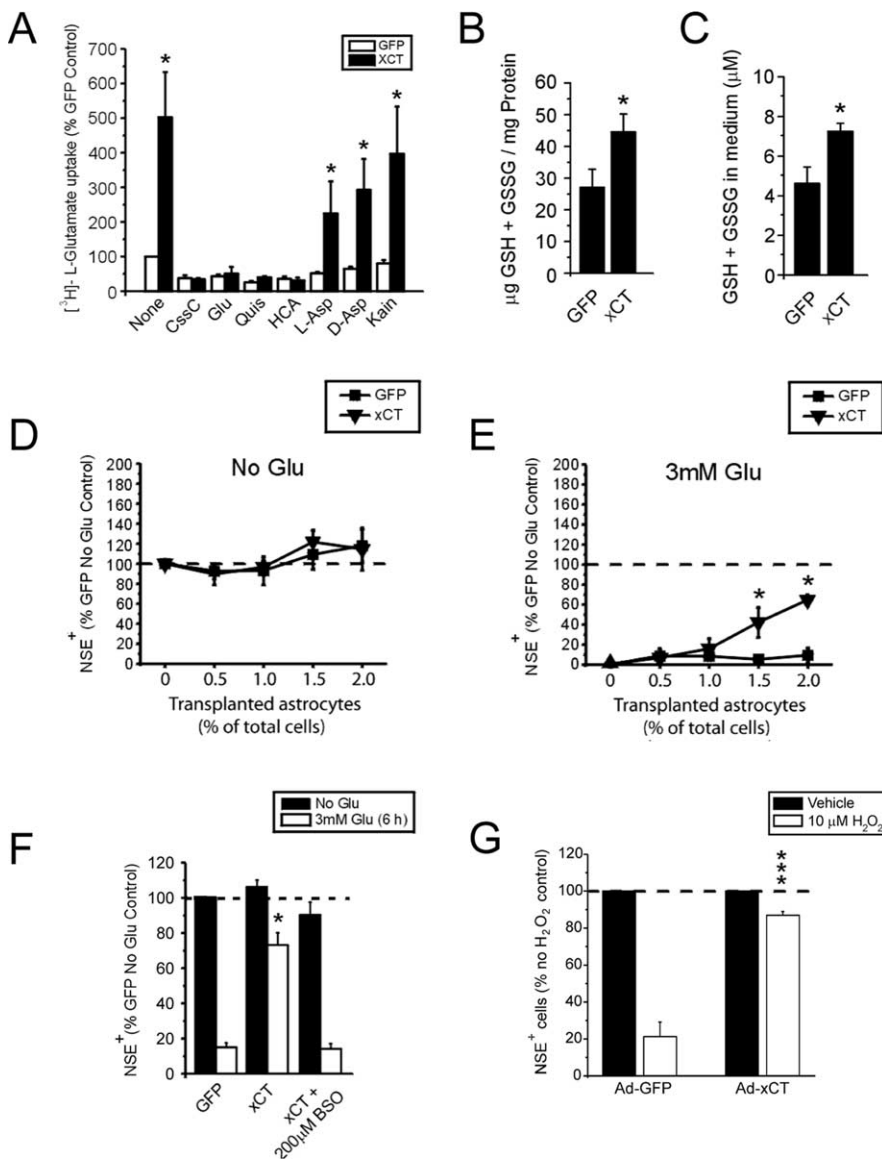
Figure 4. xCT overexpression in astrocytes enhances system x_c^- activity, increases GSH synthesis, and provides neuroprotection in a dose-dependent manner. **A**, Ad-xCT-infected mixed cultures exhibited an approximate fivefold higher Na^+-independent L-[^{3}H]glutamate uptake than Ad-GFP-infected control cultures. Enhanced uptake fit the pharmacological profile previously defined for system x_c^-. CssC, L-Cystine; Glu, L-glutamate; Quis, quisqualic acid; HCA, homocysteic acid; L-Asp, L-aspartate; D-Asp, D-aspartate; Kain, kainic acid. All competitors were introduced at a concentration of 1 mM, except quisqualic acid (300 μM). **B**, **C**, Ad-xCT infection increased total intracellular GSH and GSH in the media by ~1.7-fold and ~1.6-fold, respectively, compared with Ad-GFP control. **D**, **E**, Ad-xCT-infected astrocytes were transplanted into naive immature cortical neuron cultures and exposed to oxidative glutamate (Glu) toxicity. Ad-xCT-infected astrocytes, seeded at 2% of the total cell number, were capable of providing widespread neuronal protection. Ad-GFP-infected astrocytes were relatively not neuroprotective at the same density. **F**, GSH production was essential for neuroprotection because pretreatment of the by Ad-xCT-infected astrocytes with 200 μM BSO (an irreversible γ-glutamylcysteine synthetase inhibitor) abolished subsequent xCT-mediated neuroprotection. **G**, Ad-xCT-infected astrocytes (transplanted at 2% of total cell number) also conferred neuroprotection from direct exposure to the reactive O_2 species, H_2O_2 (10 μM for 24 h). Data represent the mean ± SEM from at least three independent experiments on separately prepared cultures. *$p < 0.05$ or ***$p < 0.001$ compared with Ad-GFP-infected astrocytes.

xCT overexpression is sufficient to enhance GSH synthesis and confer neuroprotection from oxidative stress

Because Nrf2 upregulates numerous antioxidant/detoxification genes (in addition to those involved in GSH production), neuroprotection by meningeal cells could be attributable to other Nrf2-regulated pathways. Thus, we examined whether increased xCT activity alone was sufficient to confer neuroprotection from oxidative stress using ectopic xCT overexpression. 4F2hc was not concomitantly overexpressed because it had the potential to affect the transport activities of other glycoprotein-associated transporters and may be unnecessary because of adequate endogenous 4F2hc expression (Shih and Murphy, 2001). Ad-xCT-infected astrocyte cultures exhibited fivefold higher Na^+-independent L-[^{3}H]glutamate uptake over Ad-GFP-infected controls, which fit the pharmacological profile defined for system x_c^-, as described above (Fig. 4A). Ad-xCT infection of astrocytes also increased total intracellular GSH by ~1.7-fold and GSH in the astrocyte-conditioned medium by ~1.6-fold compared with Ad-GFP control (Fig. 4B,C).

To examine the neuroprotective potential of increased xCT activity, we transplanted Ad-GFP- or Ad-xCT-infected astrocytes into naive (no virus treatment) immature cortical neuron cultures at 0–2% of the total cell number (Shih et al., 2003). The use of astrocyte transplantation avoids direct infection of neurons and isolates the specific contribution of infected astrocytes. These cocultures were then exposed to oxidative glutamate toxicity. Ad-xCT-infected astrocytes transplanted at only 2% of the total cell number conferred dose-dependent and widespread neuroprotection (Fig. 4D,E). At these seeding densities, Ad-GFP-infected astrocytes offered no neuroprotection. GSH synthesis was necessary for neuroprotection because pretreatment of Ad-xCT-infected astrocytes with the selective GSH synthesis inhibitor BSO (in separate membrane-delimited inserts) completely blocked neuroprotection (Fig. 4F). Importantly, Ad-xCT-infected astrocytes also conferred neuroprotection during direct exposure to the reactive O_2 species, H_2O_2, which does not rely on xCT inhibition to induce oxidative stress (Fig. 4G). Strikingly, Ad-xCT infection was even sufficient to enhance neuroprotective potential of fibroblasts, a cell type that is not associated with CNS neuroprotection (Fig. 5A,B). Fibroblasts infected with the Ad-GFP control virus were not neuroprotective.

Loss of xCT function inhibits astrocyte and meningeal cell proliferation *in vitro* and leads to brain atrophy *in vivo*

Recent studies have selectively linked the mouse subtle gray pigmentation mutant phenotype (sut/sut) to a truncation mutation in the xCT gene (*Slc7a11*), leading to expression of a nonfunctional xCT protein (Chintala et al., 2005). Melanocytes isolated from sut/sut mice have extremely low levels of GSH and cannot be grown under normal culture conditions unless in the presence of β-ME, a reducing agent (Chintala et al., 2005). β-ME circumvents loss of xCT function by decreasing oxidative stress and
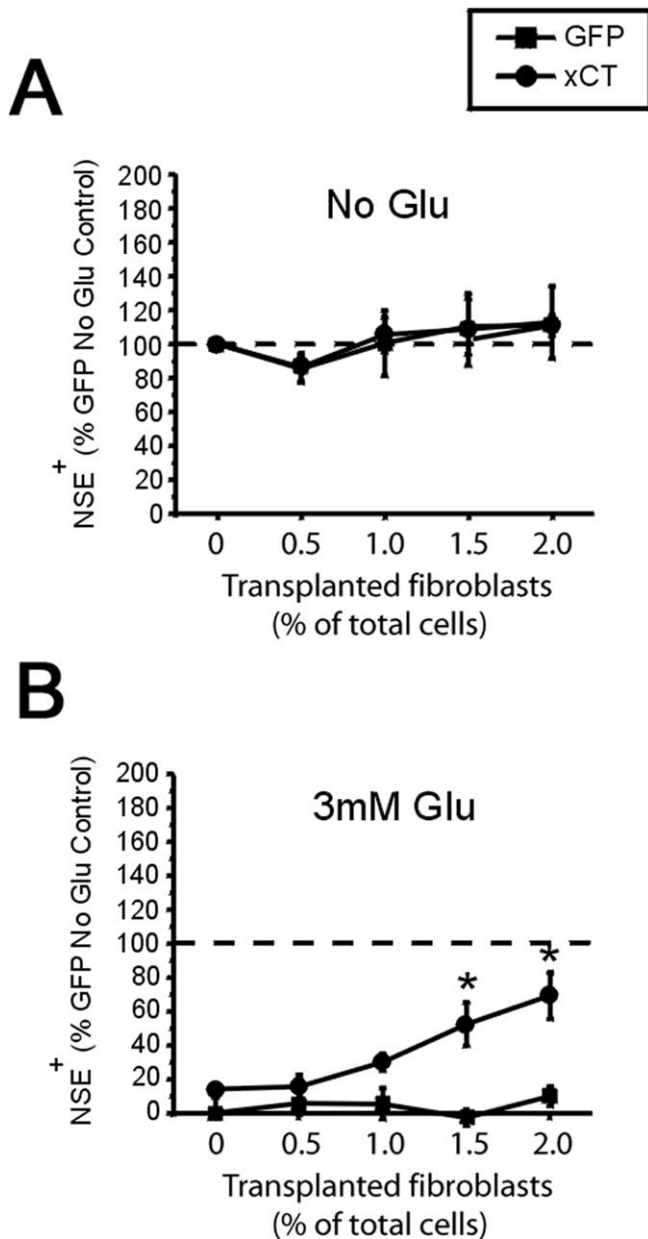
Figure 5. xCT-overexpressing fibroblasts confer neuroprotection during oxidative glutamate toxicity. Ad-xCT-infected fibroblasts were transplanted into naive immature cortical neuron cultures and exposed to oxidative glutamate toxicity (**A**, **B**; as described in Fig. 4 D, E). xCT overexpression was sufficient to increase neuroprotection by fibroblasts, a cell type that was not associated with CNS neuroprotection. Ad-GFP-infected fibroblasts were relatively not neuroprotective in comparison. Data represent the mean ± SEM from three independent experiments on separately prepared cultures. *$p < 0.05$ compared with Ad-GFP-infected fibroblasts.
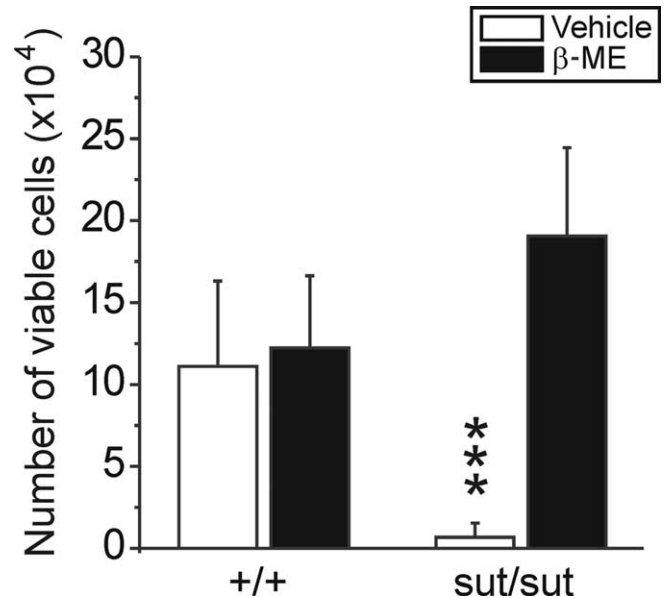

Figure 6. Astrocytes derived from sut/sut mice are unable to proliferate early in culture. Astrocyte cultures were prepared from P0–P2 sut/sut mouse pups (sut/sut) or C3H/HeSnJ controls (+/+). After 7 DIV, total viable cells from each well of a 12-well plate were counted using Trypan blue exclusion. Under normal culture conditions, sut/sut astrocytes were unable to proliferate, whereas +/+ astrocytes grew normally. The application of 55 μM β-ME to the culture medium rescued sut/sut astrocyte growth but had no significant effect on +/+ astrocytes. Data represent the mean ± SEM from three independent experiments on separately prepared cultures. ***$p < 0.001$ compared with sut/sut astrocytes with β-ME treatment.

reducing extracellular cystine to cysteine for uptake by other non-xCT transport systems. Consistent with these results, we found that astrocytes cultured from sut/sut mouse pups failed to proliferate unless cultured with β-ME from the day of plating (0 DIV) (Fig. 6). In contrast, astrocytes derived from the control C3H/HeSnJ (+/+) background strain proliferated normally with and without β-ME (Fig. 6). Meningeal cells from sut/sut mice were also unable to proliferate without β-ME (data not shown). Interestingly, our preliminary results suggest that β-ME is only necessary during the initial stages of culturing. Removal of β-ME after 1 week of culture did not affect sut/sut astrocyte viability or GSH content (data not shown), suggesting that im-

mature proliferating astrocytes rely on xCT, whereas mature astrocytes adapt to use other mechanisms of cyst(e)ine uptake or induce antioxidant factors that allow them to cope with stressful conditions. Unfortunately, the requirement of β-ME early in culture to prevent astrocyte cell death would make it difficult to interpret the role of xCT loss of function in direct protection of neurons in a coculture experiment (as in Figs. 4 and 5).

Our results show that xCT is widely expressed in the mature brain and its function is important for astrocyte and meningeal cell proliferation *in vitro*. We therefore reasoned that loss of xCT activity could alter the development of the sut/sut mouse brain. We compared gross brain morphology on coronal sections between adult sut/sut and +/+ mice (Fig. 7A). When examined at comparable ages (+/+, 13.5 ± 1.2 weeks; sut/sut, 13.7 ± 0.1 weeks), sut/sut mice exhibited no difference in body weight compared with controls (+/+, 28.0 ± 0.5 g; sut/sut, 28.1 ± 1.7 g). However, brain size was significantly reduced indicating atrophy in certain brain tissues (Fig. 6B) (reduced hemispheric area; **$p < 0.0057$). Indeed, sut/sut mice exhibited pronounced enlargement of the ventricles (Fig. 6C) (***$p < 0.0001$), accompanied by thinning of the cortex (Fig. 6D) (*$p < 0.0059$) and shrinkage of the striatum (Fig. 6E) (*$p < 0.023$). A trend toward shrinkage of hippocampus was observed, particularly in the posterior regions. However, this difference was not significant in statistical analysis (Fig. 6F) ($p = 0.34$).

Discussion

We show that enhanced xCT activity in astrocytes is sufficient to increase GSH synthesis/release and protect cocultured neurons during oxidative stress-based toxicity *in vitro*. Meningeal cells naturally exhibit high levels xCT-mediated GSH production and may provide a reservoir for GSH *in vivo*. Fibroblasts, a cell type not associated with CNS neuroprotection, could be re-
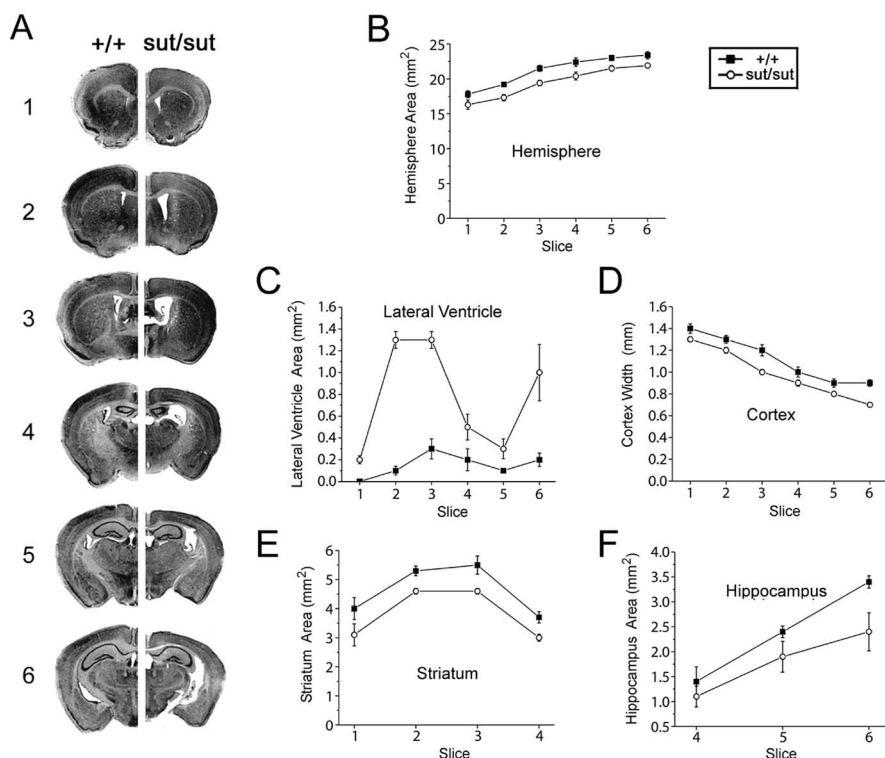
Figure 7. Adult sut/sut mice exhibit brain atrophy. **A**, Gross brain morphology was compared between cresyl violet-stained coronal sections from sut/sut mice (sut/sut) ($n = 7$; 3 males and 4 females) and C3H/HeSnJ controls ($+/+$) ($n = 6$; 3 males and 3 females). **B**, **C**, sut/sut mice exhibited an overall smaller brain size (**B**; $p = 0.0057$) and severely enlarged lateral ventricles (**C**; $p < 0.0001$). **D**, **E**, Furthermore, we observed cortical thinning (**D**; $p = 0.0059$) and reduced striatal area (**E**; $p = 0.023$). **F**, No significant difference, however, was seen in the hippocampal area, although a trend was noted ($p = 0.34$). Data represent the mean $\pm$ SEM. All statistical analyses were performed with two-way ANOVA; $p < 0.05$ was considered statistically significant.

engineered to be neuroprotective with xCT overexpression. Our results also reveal a role for xCT in brain cell proliferation *in vitro* and possibly *in vivo*. Astrocytes and meningeal cells derived from sut/sut mice show greatly reduced proliferation because of increased oxidative stress. sut/sut mice show brain atrophy by early adulthood, exhibiting enlarged ventricles, cortical thinning, and striatal shrinkage.

Role of xCT at the CSF–brain barrier

xCT protein was most highly expressed at structures forming the CSF–blood–brain barrier (meninges and periventricular zone), in agreement with previous studies (Sato et al., 2002; Burdo et al., 2006). Based on this unique localization, Bannai and colleagues (Sato et al., 2002) proposed a role for xCT in recycling cystine to cysteine in the CSF and plasma to maintain redox balance. This is plausible because cystine is the predominant sulfhydryl species extracted from plasma by brain (Wang and Cynader, 2000). Furthermore, cystine levels in the CSF and plasma are very low (micromolar range), suggesting that a high-affinity transport system such as xCT would be necessary (Gjessing et al., 1972; Perry et al., 1975). Indeed, targeted deletion of the mouse xCT gene led to higher cystine/cysteine ratios in blood plasma *in vivo* (Sato et al., 2005).

Consistent with xCT localization, our previous examination of GSH distribution in brain slices also revealed the highest GSH levels in cells of the leptomeninges and ventricular ependyma, even when compared with cortical astrocytes (Sun et al., 2006). Because GSH efflux is dependent on intracellular GSH content, these sites may support neuronal viability by releasing GSH to

distant sites within the brain (Sagara et al., 1996). Here we reconstitute this mechanism *in vitro*, with meningeal cells conferring widespread protection of immature neurons in a coculture system. Although there are several steps in the pathway to GSH synthesis, we show that xCT is rate limiting because xCT overexpression alone (in astrocytes or fibroblasts) was sufficient to increase GSH synthesis/release and confer neuroprotection.

Role of xCT in astrocyte–neuron GSH coupling and neuroprotection

Our data also suggest that xCT protein is widely expressed in other brain structures including the cortex, hippocampus, striatum, and cerebellum, albeit at much lower levels than meningeal tissue. For this work, we used Western blot because we could confidently distinguish bands representing xCT from those that were nonspecific using standards derived from cultures overexpressing xCT. Although our antibody exhibited nonspecific reactivity in Western blots (95 kDa band), there is no evidence that this is a problem for *in situ* immunostaining performed in other studies. With caveats in mind, we had previously detected xCT expression primarily in neurons of the prefrontal cortex (Melendez et al., 2005). However, in a more detailed analyses with another peptide-directed xCT antibody, Burdo et al. (2006) also found xCT expression in both MAP2 (microtubule-associated protein-2)-positive neurons and GFAP-positive astrocytes of the adult mouse cortex. A large body of *in vitro* data show that system x_c^- activity can exist in mature astrocytes and immature neurons (Murphy et al., 1990; Sagara et al., 1993a,b; Kranich et al., 1998; Schubert and Piasecki, 2001; Lewerenz et al., 2003). We also detected significant xCT-dependent L-[^{35}S]cystine uptake in cultured astrocytes (Fig. 2C). However, cyst(e)ine supply remains a limiting factor for GSH synthesis in astrocytes because xCT overexpression continues to increase GSH synthesis/release. Similarly, because cystine (and not cysteine) is most readily available in culture media, it is logical to expect that increased xCT activity in mature neurons would promote neuronal GSH synthesis and neuroprotection. Unfortunately, we could not perform this experiment using Ad-xCT because the adenovirus has poor tropism for mature neurons.

Given that astrocyte-specific enhancement of xCT activity promotes neuroprotective GSH coupling between astrocyte and immature neurons in a coculture system, targeted and controlled xCT expression/induction may be a strategy to achieve neuroprotection *in vivo*. Although xCT is only one of many Phase 2 genes regulated by Nrf2, our *in vitro* results show that xCT overexpression alone is sufficient to partially recapitulate the neuroprotective potential of Nrf2, at least with the toxicity paradigms we have examined (Ishii et al., 1999; Sasaki et al., 2002; Shih et al., 2003). To dissociate the role of xCT-mediated neuroprotection *in vivo*, future studies could examine whether loss of xCT function in sut/sut mice blunts the effect of Nrf2-inducing electrophilic

agents during *in vivo* toxicity and injury models (Shih et al., 2005a,b; Satoh et al., 2006).

Controlling glutamate release with enhanced xCT activity

Increasing cystine–glutamate exchange can potentially lead to release of excitotoxic amounts of glutamate because extracellular cystine is exchanged for intracellular glutamate (Warr et al., 1999). For example, glioma cells exhibit particularly high amounts of system x_c^- activity but low Na^+-dependent glutamate transport activity (Ye et al., 1999; Chung et al., 2005). In these extreme circumstances, release of glutamate by xCT and its excitotoxic effect on surrounding neurons is thought to facilitate growth of gliomas *in vivo*. It is also conceivable that gliomas require high xCT activity because they are under continuous oxidative stress as a result of their rapid growth. xCT activity in microglia and macrophages may also increase cytotoxicity through release of glutamate (Piani and Fontana, 1994; Barger and Basile, 2001). Thus, induction of xCT activity as a neuroprotective strategy should be targeted to enhance the neurosupportive role of astrocyte/meningeal cells, in which glutamate efflux may be better controlled. There is evidence suggesting that xCT expression is normally coregulated with high-affinity Na^+-dependent glutamate transporters that reuptake glutamate released by xCT to both minimize extracellular accumulation and maintain adequate glutamate driving force for xCT activity (Lewerenz et al., 2006). Indeed, control mechanisms may exist *in vivo* because astrocytes are well known to express high-affinity glutamate transporters GLAST and GLT-1 (Danbolt, 2001).

Role of xCT in brain cell growth and proliferation

The rate of cell proliferation is strongly associated with cyst(e)ine availability and intracellular GSH content (Godwin et al., 1992; Noda et al., 2002). For example, continuous proliferation of cancer cells is associated with high oxidative load, and pharmacological blockade of xCT inhibits growth of various cancer cell types by depleting GSH (Uren and Lazarus, 1979; Gout et al., 2001; Chung et al., 2005). Our results show that astrocytes and meningeal cells derived from sut/sut mice were unable to grow *in vitro* without the presence of β-ME (Chintala et al., 2005). However, unlike other cell types derived from xCT-deficient mice (i.e., melanocytes and fibroblasts) (Chintala et al., 2005; Sato et al., 2005), subsequent removal of β-ME after 7 d of growth did not decrease GSH content or cell viability. Thus, astrocytes may adapt to have complementary cyst(e)ine transport mechanisms during maturation (i.e., system x_{AG} and ASC) (Cho and Bannai, 1990; Bender et al., 2000; Allen et al., 2002; McBean, 2002). It is also possible that mature astrocytes are quiescent and do not require high levels of GSH. Accordingly, GSH content and viability of mature astrocytes are primarily unaffected by treatment with millimolar levels of glutamate or sulfasalazine, two treatments known to block xCT transport (Shih et al., 2003; Chung et al., 2005).

Interestingly, immature neurons and oligodendrocyte precursors are also highly sensitive to cystine deprivation *in vitro* (Murphy et al., 1990; Sagara et al., 1993a; Back et al., 1998), suggesting a critical developmental role for xCT that may apply to multiple brain cell types. We previously hypothesized that high xCT expression and GSH content in the lateral ventricular ependyma may be uniquely positioned to support proliferation of neuronal progenitors in the subventricular zone *in vivo* (Sun et al., 2006). Studies using the transplantation of neuronal stem cells may benefit from xCT-dependent manipulation of high-affinity cystine uptake for GSH synthesis.

We also observed brain atrophy in sut/sut mice by early adulthood. Future studies will examine when these morphological changes begin and what brain regions/cells are most dependent on xCT *in vivo*. Because immature brain cells appear to be most sensitive to xCT blockade *in vitro*, we speculate that atrophy begins at the embryonic to perinatal stage (Murphy et al., 1990). Loss of xCT function may impede GSH synthesis necessary for detoxifying metabolic byproducts and oxidative stressors produced during cell proliferation and maturation, possibly leading to cell death during development (Lowndes et al., 1994). Notably, the morphological changes observed in sut/sut mice brains bear remarkable similarities to aged EAAC1 knock-out mice, where brain atrophy is caused by age-dependent thiol depletion and toxicity of mature neurons. The fact that we see obvious differences at 3.5 months, a relatively young age compared with the aged EAAC1 knock-out mice examined in their study (11 months), further suggests that disturbances occur early in development (Aoyama et al., 2005).

References

Allen JW, Shanker G, Tan KH, Aschner M (2002) The consequences of methylmercury exposure on interactive functions between astrocytes and neurons. Neurotoxicology 23:755–759.

Aoyama K, Suh SW, Hamby AM, Liu J, Chan WY, Chen Y, Swanson RA (2006) Neuronal glutathione deficiency and age-dependent neurodegeneration in the EAAC1 deficient mouse. Nat Neurosci 9:119–126.

Back SA, Gan X, Li Y, Rosenberg PA, Volpe JJ (1998) Maturation-dependent vulnerability of oligodendrocytes to oxidative stress-induced death caused by glutathione depletion. J Neurosci 18:6241–6253.

Barger SW, Basile AS (2001) Activation of microglia by secreted amyloid precursor protein evokes release of glutamate by cystine exchange and attenuates synaptic function. J Neurochem 76:846–854.

Bender AS, Reichelt W, Norenberg MD (2000) Characterization of cystine uptake in cultured astrocytes. Neurochem Int 37:269–276.

Bobyn PJ, Franklin JL, Wall CM, Thornhill JA, Juurlink BH, Paterson PG (2002) The effects of dietary sulfur amino acid deficiency on rat brain glutathione concentration and neural damage in global hemispheric hypoxia-ischemia. Nutr Neurosci 5:407–416.

Burdo J, Dargusch R, Schubert D (2006) Distribution of the cystine/glutamate antiporter system xc- in the brain, kidney, and duodenum. J Histochem Cytochem 54:549–557.

Chan K, Lu R, Chang JC, Kan YW (1996) NRF2, a member of the NFE2 family of transcription factors, is not essential for murine erythropoiesis, growth, and development. Proc Natl Acad Sci USA 93:13943–13948.

Chatterjee S, Noack H, Possel H, Keilhoff G, Wolf G (1999) Glutathione levels in primary glial cultures: monochlorobimane provides evidence of cell type-specific distribution. Glia 27:152–161.

Chen Y, Swanson RA (2003) The glutamate transporters EAAT2 and EAAT3 mediate cysteine uptake in cortical neuron cultures. J Neurochem 84:1332–1339.

Chintala S, Li W, Lamoreux ML, Ito S, Wakamatsu K, Sviderskaya EV, Bennett DC, Park YM, Gahl WA, Huizing M, Spritz RA, Ben S, Novak EK, Tan J, Swank RT (2005) Slc7a11 gene controls production of pheomelanin pigment and proliferation of cultured cells. Proc Natl Acad Sci USA 102:10964–10969.

Cho Y, Bannai S (1990) Uptake of glutamate and cysteine in C-6 glioma cells and in cultured astrocytes. J Neurochem 55:2091–2097.

Chung WJ, Lyons SA, Nelson GM, Hamza H, Gladson CL, Gillespie GY, Sontheimer H (2005) Inhibition of cystine uptake disrupts the growth of primary brain tumors. J Neurosci 25:7101–7110.

Danbolt NC (2001) Glutamate uptake. Prog Neurobiol 65:1–105.

Dringen R, Gutterer JM, Hirrlinger J (2000) Glutathione metabolism in brain metabolic interaction between astrocytes and neurons in the defense against reactive oxygen species. Eur J Biochem 267:4912–4916.

Gjessing LR, Gjesdahl P, Sjaastad O (1972) The free amino acids in human cerebrospinal fluid. J Neurochem 19:1807–1808.

Gochenauer GE, Robinson MB (2001) Dibutyryl-cAMP (dbcAMP) upregulates astrocytic chloride-dependent L-[3H]glutamate transport and expression of both system xc(-) subunits. J Neurochem 78:276–286.

Godwin AK, Meister A, O'Dwyer PJ, Huang CS, Hamilton TC, Anderson ME (1992) High resistance to cisplatin in human ovarian cancer cell lines is

associated with marked increase of glutathione synthesis. Proc Natl Acad Sci USA 89:3070–3074.

Gout PW, Buckley AR, Simms CR, Bruchovsky N (2001) Sulfasalazine, a potent suppressor of lymphoma growth by inhibition of the x(c)- cystine transporter: a new action for an old drug. Leukemia 15:1633–1640.

Hardy S, Kitamura M, Harris-Stansil T, Dai Y, Phipps ML (1997) Construction of adenovirus vectors through Cre-lox recombination. J Virol 71:1842–1849.

Ishii T, Itoh K, Sato H, Bannai S (1999) Oxidative stress-inducible proteins in macrophages. Free Radic Res 31:351–355.

Kim JY, Kanai Y, Chairoungdua A, Cha SH, Matsuo H, Kim DK, Inatomi J, Sawa H, Ida Y, Endou H (2001) Human cystine/glutamate transporter: cDNA cloning and upregulation by oxidative stress in glioma cells. Biochim Biophys Acta 1512:335–344.

Kranich O, Dringen R, Sandberg M, Hamprecht B (1998) Utilization of cysteine and cysteine precursors for the synthesis of glutathione in astroglial cultures: preference for cystine. Glia 22:11–18.

Lewerenz J, Letz J, Methner A (2003) Activation of stimulatory heteromeric G proteins increases glutathione and protects neuronal cells against oxidative stress. J Neurochem 87:522–531.

Lewerenz J, Klein M, Methner A (2006) Cooperative action of glutamate transporters and cystine/glutamate antiporter system X protects from oxidative glutamate toxicity. J Neurochem 98:916–925.

Li Y, Maher P, Schubert D (1997) Requirement for cGMP in nerve cell death caused by glutathione depletion. J Cell Biol 139:1317–1324.

Lowndes HE, Beiswanger CM, Philbert MA, Reuhl KR (1994) Substrates for neural metabolism of xenobiotics in adult and developing brain. Neurotoxicology 15:61–73.

Mastroberardino L, Spindler B, Pfeiffer R, Skelly PJ, Loffing J, Shoemaker CB, Verrey F (1998) Amino-acid transport by heterodimers of 4F2hc/CD98 and members of a permease family. Nature 395:288–291.

McBean GJ (2002) Cerebral cystine uptake: a tale of two transporters. Trends Pharmacol Sci 23:299–302.

Meister A, Anderson ME (1983) Glutathione. Annu Rev Biochem 52:711–760.

Melendez RI, Vuthiganon J, Kalivas PW (2005) Regulation of extracellular glutamate in the prefrontal cortex: focus on the cystine glutamate exchanger and group I metabotropic glutamate receptors. J Pharmacol Exp Ther 314:139–147.

Miura K, Ishii T, Sugita Y, Bannai S (1992) Cystine uptake and glutathione level in endothelial cells exposed to oxidative stress. Am J Physiol 262:C50–C58.

Mizui T, Kinouchi H, Chan PH (1992) Depletion of brain glutathione by buthionine sulfoximine enhances cerebral ischemic injury in rats. Am J Physiol 262:H313–H317.

Murphy TH, Schnaar RL, Coyle JT (1990) Immature cortical neurons are uniquely sensitive to glutamate toxicity by inhibition of cystine uptake. FASEB J 4:1624–1633.

Noda T, Iwakiri R, Fujimoto K, Rhoads CA, Aw TY (2002) Exogenous cysteine and cystine promote cell proliferation in CaCo-2 cells. Cell Prolif 35:117–129.

Patel SA, Warren BA, Rhoderick JF, Bridges RJ (2004) Differentiation of substrate and non-substrate inhibitors of transport system xc(-): an obligate exchanger of L-glutamate and L-cystine. Neuropharmacology 46:273–284.

Perry TL, Hansen S, Kennedy J (1975) CSF amino acids and plasma–CSF amino acid ratios in adults. J Neurochem 24:587–589.

Piani D, Fontana A (1994) Involvement of the cystine transport system xc- in the macrophage-induced glutamate-dependent cytotoxicity to neurons. J Immunol 152:3578–3585.

Pow DV (2001) Visualising the activity of the cystine-glutamate antiporter in glial cells using antibodies to aminoadipic acid, a selectively transported substrate. Glia 34:27–38.

Ratan RR, Murphy TH, Baraban JM (1994) Oxidative stress induces apoptosis in embryonic cortical neurons. J Neurochem 62:376–379.

Sagara J, Miura K, Bannai S (1993a) Cystine uptake and glutathione level in fetal brain cells in primary culture and in suspension. J Neurochem 61:1667–1671.

Sagara JI, Miura K, Bannai S (1993b) Maintenance of neuronal glutathione by glial cells. J Neurochem 61:1672–1676.

Sagara J, Makino N, Bannai S (1996) Glutathione efflux from cultured astrocytes. J Neurochem 66:1876–1881.

Sasaki H, Sato H, Kuriyama-Matsumura K, Sato K, Maebara K, Wang H, Tamba M, Itoh K, Yamamoto M, Bannai S (2002) Electrophile response element-mediated induction of the cystine/glutamate exchange transporter gene expression. J Biol Chem 277:44765–44771.

Sato H, Tamba M, Ishii T, Bannai S (1999) Cloning and expression of a plasma membrane cystine/glutamate exchange transporter composed of two distinct proteins. J Biol Chem 274:11455–11458.

Sato H, Tamba M, Okuno S, Sato K, Keino-Masu K, Masu M, Bannai S (2002) Distribution of cystine/glutamate exchange transporter, system xc-, in the mouse brain. J Neurosci 22:8028–8033.

Sato H, Shiiya A, Kimata M, Maebara K, Tamba M, Sakakura Y, Makino N, Sugiyama F, Yagami K, Moriguchi T, Takahashi S, Bannai S (2005) Redox imbalance in cystine/glutamate transporter-deficient mice. J Biol Chem 280:37423–37429.

Satoh T, Okamoto SI, Cui J, Watanabe Y, Furuta K, Suzuki M, Tohyama K, Lipton SA (2006) Activation of the Keap1/Nrf2 pathway for neuroprotection by electrophillic phase II inducers. Proc Natl Acad Sci USA 103:768–773.

Schubert D, Piasecki D (2001) Oxidative glutamate toxicity can be a component of the excitoxicity cascade. J Neurosci 21:7455–7462.

Shanker G, Allen JW, Mutkus LA, Aschner M (2001) The uptake of cysteine in cultured primary astrocytes and neurons. Brain Res 902:156–163.

Shih AY, Murphy TH (2001) xCt cystine transporter expression in HEK293 cells: pharmacology and localization. Biochem Biophys Res Commun 282:1132–1137.

Shih AY, Johnson DA, Wong G, Kraft AD, Jiang L, Erb H, Johnson JA, Murphy TH (2003) Coordinate regulation of glutathione biosynthesis and release by Nrf2-expressing glia potently protects neurons from oxidative stress. J Neurosci 23:3394–3406.

Shih AY, Imbeault S, Barakauskas V, Erb H, Jiang L, Li P, Murphy TH (2005a) Induction of the Nrf2-driven antioxidant response confers neuroprotection during mitochondrial stress in vivo. J Biol Chem 280:22925–22936.

Shih AY, Li P, Murphy TH (2005b) A small-molecule-inducible Nrf2-mediated antioxidant response provides effective prophylaxis against cerebral ischemia in vivo. J Neurosci 25:10321–10335.

Sun X, Erb H, Murphy TH (2005) Coordinate regulation of glutathione metabolism in astrocytes by Nrf2. Biochem Biophys Res Commun 326:371–377.

Sun X, Shih AY, Johannssen HC, Erb H, Li P, Murphy TH (2006) Two-photon imaging of glutathione levels in intact brain indicates enhanced redox buffering in developing neurons and cells at the cerebrospinal fluid and blood-brain interface. J Biol Chem 281:17420–17431.

Szumlinski KK, Dehoff MH, Kang SH, Frys KA, Lominac KD, Klugmann M, Rohrer J, Griffin III W, Toda S, Champtiaux NP, Berry T, Tu JC, Shealy SE, During MJ, Middaugh LD, Worley PF, Kalivas PW (2004) Homer proteins regulate sensitivity to cocaine. Neuron 43:401–413.

Tietze F (1969) Enzymic method for quantitative determination of nanogram amounts of total and oxidized glutathione: applications to mammalian blood and other tissues. Anal Biochem 27:502–522.

Uren JR, Lazarus H (1979) L-cyst(e)ine requirements of malignant cells and progress toward depletion therapy. Cancer Treat Rep 63:1073–1079.

Wang H, Tamba M, Kimata M, Sakamoto K, Bannai S, Sato H (2003) Expression of the activity of cystine/glutamate exchange transporter, system x(c)(-), by xCT and rBAT. Biochem Biophys Res Commun 305:611–618.

Wang XF, Cynader MS (2000) Astrocytes provide cysteine to neurons by releasing glutathione. J Neurochem 74:1434–1442.

Warr O, Takahashi M, Attwell D (1999) Modulation of extracellular glutamate concentration in rat brain slices by cystine-glutamate exchange. J Physiol (Lond) 514:783–793.

Ye ZC, Rothstein JD, Sontheimer H (1999) Compromised glutamate transport in human glioma cells: reduction–mislocalization of sodium-dependent glutamate transporters and enhanced activity of cystine–glutamate exchange. J Neurosci 19:10767–10777.

Supplemental data

- supplemental material - Supplementary Figure 1. Verification of xCT band migration
using HA-tagged xCT and Nrf2 knockout tissues. A, To verify xCT molecular weight in Western blot, HA-tagged xCT was expressed in HEK293 cells and cell lysates were probed with anti-HA and anti-4F2hc antibodies. Monomeric HA-xCT was observed as a 35 kDa and 55 kDa band, consistent with the peptide-derived xCT antibody. The 105 kDa band corresponding to the HA-xCT-4F2hc heterodimer could be disrupted under reducing conditions (-ME + dithiothreitol), as observed with both HA and 4F2hc antibodies. The 55 kDa HA-xCT band referred to as xCT-mod could not be disrupted by reducing conditions suggesting that it is not a di-sulfide linked xCT homodimer. Blots are representative results from three independent experiments on separately prepared cultures. B, The peptide-derived xCT antibody was also used to probe brain tissues from Nrf2 wild-type and knockout mice. Consistent with the xCT-specific action of our antibody, we observed a significant reduction of xCT protein expression in meninges, and a modest reduction in cortex of Nrf2 knockout mice, compares to wild-type littermates. However, overall basal levels of xCT expression throughout other brain regions were largely unaffected by Nrf2 knockout. Hippo. = hippocampus, cerebell. = cerebellum. Data represent the mean + SEM from n = 3 separate mice from each genotype. * p < 0.05, compared to Nrf2+/+ mice.
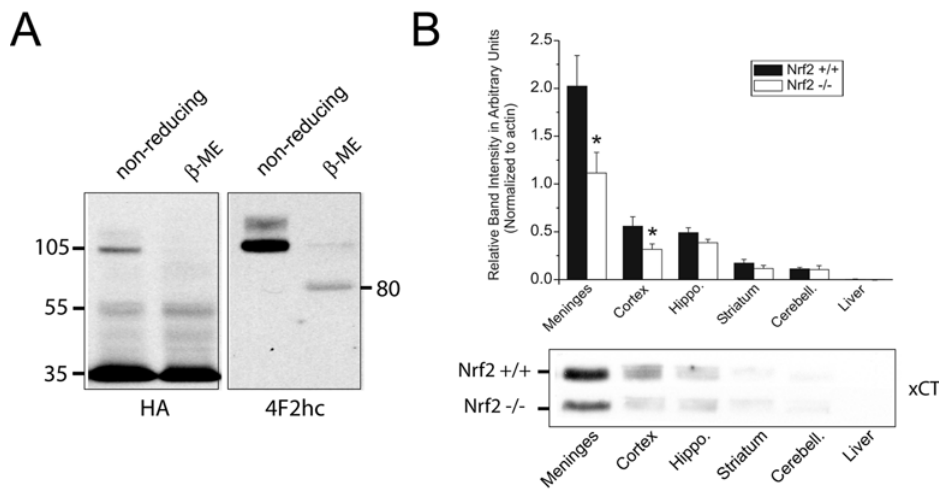
- supplemental material - Supplementary Figure 2. Total regional brain GSH levels in the embryonic and adult rat brain. A,B, Brain homogenates were collected from both age groups and assayed in the same experiment using the Tietze method (Tietze, 1969). GSH levels in embryonic brain were ~ 5x higher in all regions (note scale bars). Data represent the mean + SEM from n = 3 rats for each age group.